Mcp6, a meiosis-specific coiled-coil protein of *Schizosaccharomyces pombe*, localizes to the spindle pole body and is required for horsetail movement and recombination

Takamune T. Saito, Takahiro Tougan, Daisuke Okuzaki, Takashi Kasama and Hiroshi Nojima*

Department of Molecular Genetics, Research Institute for Microbial Diseases, Osaka University, 3-1 Yamadaoka, Suita, Osaka 565-0871, Japan

*Author for correspondence (e-mail: snj-0212@biken.osaka-u.ac.jp)

Accepted 3 November 2004
Journal of Cell Science 118, 447-459 Published by The Company of Biologists 2005
doi:10.1242/jcs.01629

Summary

We report here that a meiosis-specific gene of *Schizosaccharomyces pombe* denoted *mcp6*$^{+}$ (meiotic coiled-coil protein) encodes a protein that is required for the horsetail movement of chromosomes at meiosis I. The *mcp6*$^{+}$ gene is specifically transcribed during the horsetail phase. Green fluorescent protein (GFP)-tagged Mcp6 appears at the start of karyogamy, localizes to the spindle-pole body (SPB) and then disappears before chromosome segregation at meiosis I. In the *mcp6Δ* strain, the horsetail movement was either hampered (zygotic meiosis) or abolished (azygotic meiosis) and the pairing of homologous chromosomes was impaired. Accordingly, the allelic recombination rates of the *mcp6Δ* strain were only 10-40% of the wild-type rates. By contrast, the ectopic recombination rate of the *mcp6Δ* strain was twice the wild-type rate. This is probably caused by abnormal homologous pairing in *mcp6Δ* cells because of aberrant horsetail movement. Fluorescent microscopy indicates that SPB components such as Sad1, Kms1 and Spo15 localize normally in *mcp6Δ* cells. Because Taz1 and Swi6 also localized with Sad1 in *mcp6Δ* cells, Mcp6 is not required for telomere clustering. In a *taz1Δ* strain, which does not display telomere clustering, and the *dhc1-d3* mutant, which lacks horsetail movement, Mcp6 localized with Sad1 normally. However, we observed abnormal astral microtubule organization in *mcp6Δ* cells. From these results, we conclude that Mcp6 is necessary for neither SPB organization nor telomere clustering, but is required for proper astral microtubule positioning to maintain horsetail movement.

Supplementary material available online at
http://jcs.biologists.org/cgi/content/full/118/2/447/DC1

Key words: Meiosis, *S. pombe*, SPB, Recombination, Pairing, Horsetail

Introduction

Sexually reproducing eukaryotic organisms undergo meiosis, a special type of cell division, to generate inheritable haploid gametes from diploid parental cells. This process includes meiosis-specific events that increase genetic diversity, such as synaptonemal complex (SC) formation, homologous pairing and recombination. The fission yeast *Schizosaccharomyces pombe* proceeds to meiosis when it is nutritionally starved. At this point, two cells with opposite mating types conjugate and the two haploid nuclei fuse, thereby producing a zygote with a diploid nucleus; the meiotic process immediately follows this. Efficient pairing of the homologous chromosomes and the subsequent processing and completion of recombination during the meiotic prophase are pivotal for achieving correct chromosome segregation during meiotic division. An essential event for efficient chromosome pairing in *S. pombe* is the clustering during prophase of meiosis I of the telomeres of three chromosomes near the spindle-pole body (SPB) (Chikashige et al., 1994; Chikashige et al., 1997). This characteristic arrangement of meiotic chromosomes has been observed in a wide range of organisms and is denoted a 'bouquet' arrangement (Loidl, 1990; Scherthan, 2001; Zickler and Kleckner, 1999). This arrangement has been proposed to facilitate homologous chromosome pairing because it generates a polarized chromosome configuration by bundling chromosomes together at their telomeres.

The clustering of telomeres occurs during an event termed horsetail nuclear movement that is characteristic of *S. pombe*. It occurs at prophase I of meiosis and is characterized by a dynamic oscillation of the nucleus and the adoption by the nucleus of an elongated morphology (Chikashige et al., 1994). This movement has been proposed to facilitate the pairing of homologous chromosomes because it causes the chromosomes, which are aligned in the same direction as a result of bundling at their telomeric ends, to be shuffled around each other (Chikashige et al., 1994; Kohli, 1994; Hiraoka, 1998; Yamamoto et al., 1999; Yamamoto and Hiraoka, 2001). Thus, it enhances the chance that a chromosome encounters its correct partner and thereby promotes the linkage of homologous pairs of chromosomes through homologous recombination. In support of this notion, homologous recombination is reduced in mutants that display impaired

telomere clustering owing to the depletion of protein components of the telomere or the SPB, even though recombination machinery is intact in these mutants. For example, elimination of the telomere-binding protein Taz1 (Cooper et al., 1998; Nimmo et al., 1998) or Rap1 (Kanoh and Ishikaw, 2001), or depletion of the SPB component Kms1 (Shimanuki et al., 1997; Niwa et al., 2000) results in a loss of telomere-SPB clustering and reduced meiotic recombination.

It has been proposed that horsetail nuclear movement is predominantly established by pulling the astral microtubules that link the SPB to microtubule-anchoring sites, and that the pulling force is provided by cytoplasmic dynein (Chikashige et al., 1994; Svoboda et al., 1995; Ding et al., 1998; Yamamoto and Hiraoka, 2003). Thus, homologous recombination is also reduced when nuclear oscillation is abolished by disrupting the *dhc1*$^+$ gene, which encodes dynein heavy chain (DHC), a major component of cytoplasmic dynein that is localized to microtubules and the SPB (Yamamoto et al., 1999). It was proposed that dynein drives this nuclear oscillation by mediating the cortical microtubule interactions and regulating the dynamics of microtubule disassembly at the cortex (Yamamoto et al., 2001). Meiotic recombination is also reduced in a null mutant of the *dlc1*$^+$ gene that encodes an SPB protein that belongs to the dynein-light-chain family (Miki et al., 2003). In this mutant, Dhc1-dependent nuclear movement during meiotic prophase is irregular in its duration and direction. This model explains some of the regulatory mechanisms behind nuclear oscillation and chromosome pairing. However, the details of these mechanisms are still mostly unknown. The identification of additional regulatory components is needed fully to elucidate these processes.

In the course of our functional characterization of meiotic-specific proteins that harbour coiled-coil motifs, we found a new SPB-associated protein that is required for meiotic nuclear oscillation and recombination. This gene is expressed specifically during meiosis and thus is referred to as *mcp6*$^+$ (meiotic coiled-coil protein). The coiled-coil motif, which consists of two to five amphipathic α-helices that twist around one another to form a supercoil, is known to be required for protein-protein interaction (Burkhard et al., 2001). In the present study, we report our functional analysis of this protein.

Materials and Methods

Yeast strains, media and molecular biology

The *S. pombe* strains used in this study are listed in Table 1. Complete media YPD or YE, the synthetic minimal medium EMM2 and the sporulation media ME or EMM2-N (1% glucose) were used (Alfa et al., 1993). Homozygous diploid strains were constructed by cell fusion. Cells were converted to protoplasts by treatment with lysing enzyme. Then, cells were fused using $CaCl_2$ and polyethylene glycol (Sipiczki and Ferenczy, 1977). Plates with EMM2 containing 1 M sorbitol were used in the cell fusion experiments. Induction of meiosis in the genetic background of the *pat1-114* mutant (Shimada et al., 2002). Northern (Watanabe et al., 2001) and western blot (Okuzaki et al., 2003) analyses were performed as described previously.

Gene disruption

To disrupt the *mcp6*$^+$ gene by replacing it with the *ura4*$^+$ gene, we used the polymerase chain reaction (PCR) to obtain a DNA fragment carrying the 5′ upstream region and 3′ downstream region of the *mcp6*$^+$ gene. For this purpose, we synthesized the following four oligonucleotides and used them as primers: mcp6-5F, 5′-GGTAC-CTTCTGGTGCCGCCGACCTTC-3′; mcp6-5R, 5′-CTCGAGAT-TAAATCAATCTGTTAATC-3′; mcp6-3F, 5′-CCCGGGGGATAGC-TATGAAACCCTGA-3′; mcp6-3R, 5′-GAGCTCTCATTTTTTT-TATAAGAAGG-3′. (The underlined sequences denote the artificially introduced restriction enzyme sites for *Kpn*I, *Xho*I, *Sma*I and *Sac*I, respectively.) These PCR products and the 1.8 kb *Hin*dIII fragment containing the *ura4*$^+$ gene (Grimm et al., 1988) were inserted into the pBluescriptII KS (+) vector via the *Kpn*I-*Xho*I, *Sma*I-*Sac*I or *Hin*dIII sites. This plasmid construct was digested with *Kpn*I and *Sac*I, and the resulting construct was introduced into the diploid strain TP4-5A/TP4-1D. The Ura$^+$ transformants were then screened by Southern blot analysis to identify the disrupted strain.

Construction of strains harbouring integrated *mcp6*$^+$-tag genes

To construct green fluorescent protein (GFP)-tagged *mcp6*$^+$ strains, we performed PCR using the wild-type (TP4-5A) genome as a template and obtained a DNA fragment carrying the open reading frame (ORF) region and the 3′ downstream region of the *mcp6*$^+$ gene. For this purpose, we synthesized the following two oligonucleotides and used them as primers: mcp6-ORF-F, 5′-CGGCGCGCCG-CATATGGAATATCAAGAAGAGGC-3′; mcp6-ORF-R, 5′-GTA-CTCGAGGCGGCCGCGGGCTCAGATCGTGATTGACAG3′. The underlined sequences denote the artificially introduced restriction enzyme sites for *Asc*I and *Nde*I, and *Xho*I and *Not*I, respectively. To obtain the 3′ downstream region, we used the same primers as described above. These PCR products were inserted into the pTT(GFP)-Lys3 vector (T.T., unpublished) (see supplementary material Fig. S1), which is designed to allow one-step integration via *Nde*I-*Not*I and *Sma*I-*Sac*I sites. This plasmid construct was digested with *Pme*I. The resulting construct was introduced into strain HM105 (*h*$^-$ *lys3*). We then screened the Lys$^+$ transformants and confirmed the precise integration of the constructs by PCR.

Recombination frequency and spore viability

The crossing-over rate was determined as described previously (Fukushima et al., 2000). Briefly, haploid parental strains were grown on YPD plates at 30°C and cells were mated and sporulated on ME plates at 28°C (zygotic meiosis). After 1 day of incubation, the spores were separated by a micromanipulator (Singer Instruments, UK). To examine the frequency of crossing over, we measured the genetic distance (in centiMorgans) between *leu1*$^+$ and *his2*$^+$, and between *lys3*$^+$ and *cdc12*$^+$. Genetic distance was calculated according to the formula $50\times[T+(6\times NPD)]\div(PD+T+NPD)$ (Perkins, 1949), where *T*, *NPD* and *PD* indicate the number of tetratypes, nonparental ditypes and parental ditypes, respectively.

Intragenic recombination rate and spore viability were determined as described previously (Shimada et al., 2002). Briefly, haploid parental strains were grown on YPD plates at 33°C. Cells were mated and sporulated on ME plates at 28°C (zygotic meiosis). After 3-4 days of incubation, spores were treated with 1% glusulase (NEN Life Science Products) for 2-3 hours at room temperature and checked under a microscope for complete digestion of contaminating vegetative cells. The glusulase-treated spores were then washed with water and used to measure the intragenic recombination rate and in the spore-viability assays. To examine the frequency of intragenic or ectopic recombination (or prototroph frequency), we used two *ade6* alleles – *ade6-M26* and *ade6-469* (Gutz, 1971) or *ade6-M26* and z7 (*ade6-469*) (Virgin and Bailey, 1998), because the reciprocal recombination between these alleles produces the *ade6*$^+$ allele.

Fluorescent microscopic observations

Cells from a single colony were cultured at 28°C in 10 ml EMM2 plus supplements [adenine (75 μg/ml), histidine (75 μ/ml), leucine (250

Table 1. Strains used in this study

Strain	Genotype	Source†
CD16-1	*h⁺/h⁻ ade6-M210/ade6-M216 cyh1/⁺ ⁺/lys5-391*	C. Shimoda (Osaka City University, Osaka, Japan)
CD16-5	*h⁻/h⁻ ade6-M210/ade6-M216 cyh1/⁺ ⁺/lys5-391*	C. Shimoda
ST194	*h⁻/h⁻ ade6-M216/210 leu1-32/leu1-32 mcp6::[mcp6-GFP-3′UTR-Lys3⁺]/mcp6::[mcp6-GFP-3′UTR-Lys3⁺] pat1-114/pat1-114*	
ST142	*h⁹⁰ ade6-M216 leu1-32 ura4-D18 mcp6::[mcp6-GFP-3′UTR-Lys3⁺] dsRed-Sad1 [::LEU2]*	
JZ670	*h⁻/h⁻ ade6-M210/ade6-M216 leu1-32/leu1-32 pat1-114/pat1-114*	M. Yamamoto (University of Tokyo, Tokyo, Japan)
TT405	*h⁻/h⁻ ade6-M216/210 leu1-32/leu1-32 ura4-D18/ura4-D18 mcp6::ura4⁺/mcp6::ura4⁺ pat1-114/pat1-114*	
CT026-1*	*h⁹⁰ leu1-32 ura4-D18 TB19::GFP-lys1⁺*	Y. Hiraoka (Kamsai Advanced Research Center, Kobe, Japan)
ST193*	*h⁹⁰ leu1-32 ura4-D18 mcp6::ura4⁺ TB19::GFP-lys1⁺*	
AY174-7B	*h⁹⁰ leu1-32 ura4-D18 ade6-M210 his7::lacI-GFP-NLS-his7⁺ lys1::lacOr-lys1⁺*	K. Nabeshima (Stanford University, Stanford, CA) and A. Yamamoto (Kamsai Advanced Research Center, Kobe, Japan)
ST197	*h⁹⁰ leu1-32 ura4-D18 mcp6::ura4⁺ his7::lacI-GFP-NLS-his7⁺ lys1::lacOr-lys1⁺*	
TT8-1	*h⁻ ura4⁺*	
NP32-2A	*h⁺ leu1-32 his2 ura4-D18*	Nabeshiwa et al., 2001
TT232-1	*h⁺ his2 leu1-32 ura4-D18 lys3 cdc12*	
MS105-1B	*h⁻ ade6-M26 ura4-D18*	Shimada et al., 2002
MS111w1	*h⁺ ade6-469 ura4-D18 leu1-32 his2*	Shimada et al., 2002
GP1123	*h⁺ ade6-D1 ura4-D18 leu1-32 zzz7::[ade6-469 ura4⁺]*	G. Smith
TT398	*h⁻ ura4-D18 mcp6::ura4⁺*	
TT399	*h⁺ his2 leu1-32 ura4-D18 mcp6::ura4⁺*	
TT411	*h⁻ ura4-D18 mcp6::ura4⁺ cdc12 lys3*	
TT400	*h⁻ ade6-M26 ura4-D18 mcp6::ura4⁺*	
TT401	*h⁺ ade6-469 his2 leu1-32 ura4-D18 mcp6::ura4⁺*	
TT1014	*h⁺ ade6-D1 leu1-32 ura4-D18 mcp6::ura4⁺ zzz7::[ade6-469 ura4⁺]*	
TP4-5A	*h⁻ ade6-M210 ura4-D18 leu1-32*	C. Shimoda
TP4-1D	*h⁺ ade6-M216 his2 leu1-32 ura4-D18*	C. Shimoda
TT397-5A	*h⁻ ade6-M210 leu1-32 ura4-D18 mcp6::ura4⁺*	
TT397-1D	*h⁺ ade6-M216 his2 leu1-32 ura4-D18 mcp6::ura4⁺*	
CRL790	*h⁹⁰ ade6-216 leu1-32 ura4-D18 lys1 dsRed-Sad1 [::LEU2]*	Y. Hiraoka
ST148	*h⁹⁰ ade6-M216 leu1-32 ura4-D18 mcp6::ura4⁺ dsRed-Sad1[::LEU2]*	
ST176	*h⁹⁰ leu1-32 ura4-D18(or ⁺) dsRed-sad1[::LEU2] spo15-GFP::LEU2*	
ST171-1	*h⁹⁰ ade6-M210 leu1-32 ura4-D18(or ⁺) mcp6::ura4⁺ dsRed-sad1[::LEU2] spo15-GFP::LEU2*	
ST191-1	*h⁹⁰ leu1-32(or ⁺) dsRed-sad1[::LEU2] kms1::GFP::Kanr*	
ST172-1	*h⁹⁰ ura4-D18(or ⁺) mcp6::ura4+ dsRed-sad1[::LEU2] kms1::GFP::Kanr*	
ST178	*h⁹⁰ ade6-M216 leu1-32(or ⁺) ura4-D18(or ⁺) dsRed-sad1[::LEU2] Taz1::GFP::Kanr*	
ST173	*h⁹⁰ ade6-M216 ura4-D18(or ⁺) mcp6::ura4⁺ dsRed-sad1[::LEU2] Taz1::GFP::Kanr*	
ST179-1	*h⁹⁰ leu1-32 ura4-D18 dsRed-sad1[::LEU2] swi6⁺::GFP:leu2*	
ST174	*h⁹⁰ leu1-32 ura4-D18 mcp6::ura4⁺ dsRed-sad1[::LEU2] swi6⁺::GFP:leu2*	
YY105	*h⁹⁰ leu1-32 ura4-D18 lys1::nmt1pGFP-alpha2tubulin*	Y. Hiraoka
ST146	*h⁹⁰ leu1-32 ura4-D18 mcp6::ura4⁺ lys1::nmt1pGFP-alpha2tubulin*	
ST134	*h⁹⁰ ade6-M210 leu1-32 ura4-D18 mcp6::[mcp6-GFP-3′UTR-Lys3⁺]*	
ST196-1	*h⁹⁰ ade6-M210 leu1-32 dhc1-d3[LEU2] mcp6::[mcp6-GFP-3′UTR-Lys3⁺] dsRed-Sad1[::LEU2]*	
ST200	*h⁹⁰ ade6-M210 leu1-32 ura4-D18 taz1::ura4⁺ mcp6::[mcp6-GFP-3′UTR-Lys3⁺]*	

*TB19 signifies the N-terminal portion of DNA polymerase α (Ding et al., 2000).
†Unattributed strains were constructed for this study.

μg/ml), lysine (75 μg/ml) and uracil (75 μ/ml)] until they reached mid-log phase. The cells were collected by centrifugation, washed three times with 1 ml EMM2-N and then induced to enter meiosis by incubation in EMM2-N at 28°C for 6 hours. For live observations, we added 0.5 μg ml^{-1} Hoechst 33342 to 200 μl of the cells and an aliquot was observed under a fluorescence microscope (Olympus BX51).

For methanol fixation, cells were collected by aspiration through a glass filter (particle retention 1.2 μm; Whatman, Brentford, UK) that traps cells. The cells were then immediately immersed into methanol at –80°C and left overnight to fix the cells. The cells were then washed off the glass filter with distilled water and collected by centrifugation (2000 ***g***, 5 minutes), and the pellet was washed three times with PBS. 0.5 μg ml^{-1} Hoechst 33342 was added and the cells were observed under a fluorescence microscope.

For time-lapse observations, cells expressing GFP-tagged DNA polymerase α (Polα) (ST193 and CRL026-1) or cells expressing LacI-NLS-GFP and integrated LacO repeat at *lys1* locus (ST197 and AY174-7B) were cultured in 10 ml EMM2 plus supplements until they reached mid-log phase at 28°C. They were then induced to enter meiosis by incubation in EMM2-N at 28°C. After 5 hours of nitrogen starvation, the cells were put on a glass-bottomed dish whose surface was coated with 0.2% concanavalin A and images under a fluorescence microscope (Olympus IX71) were recorded every 2.5 minutes (1 second of exposure time) after the initiation of karyogamy. For observation of LacI-GFP dots, images were taken with a 0.3 second exposure at 5 minute intervals, with ten optical sections made at 0.5 μm intervals for each time point. Projected images obtained with Meta Morph software were analysed.

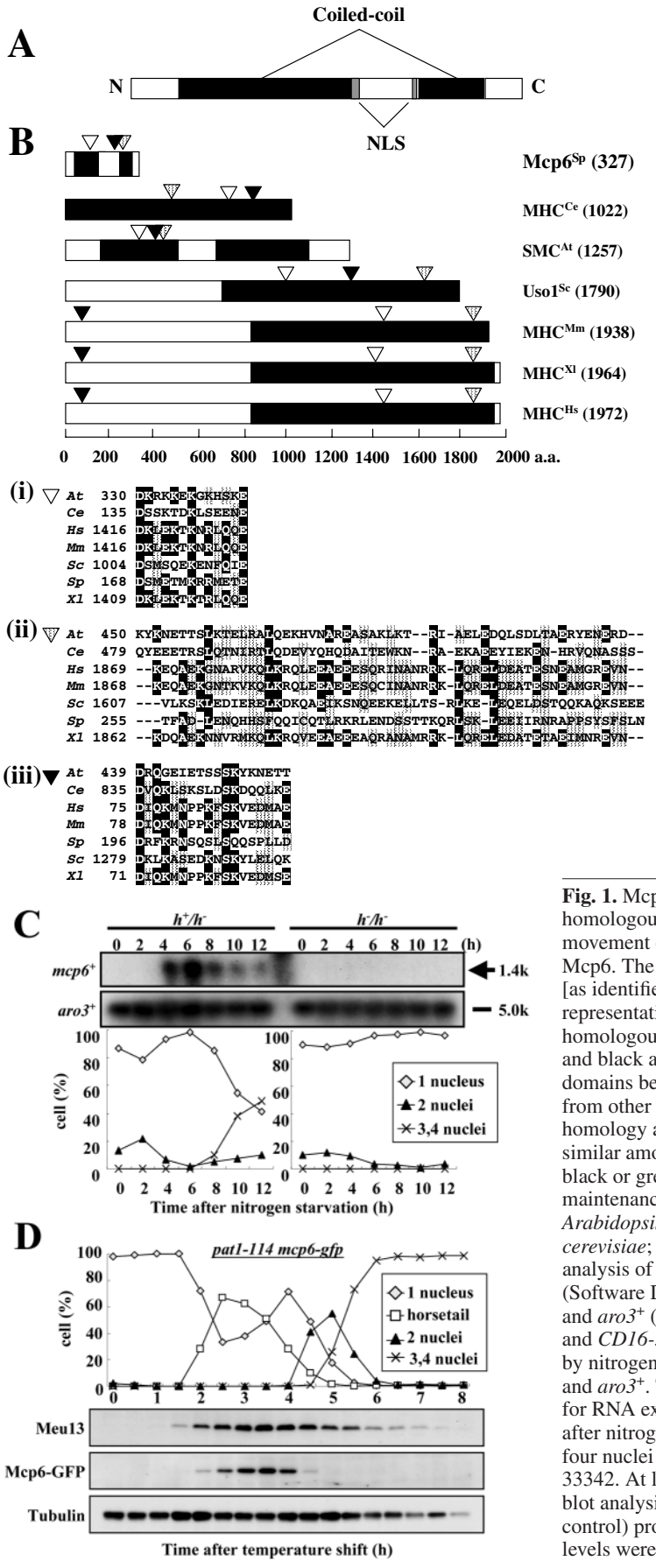

Immunofluorescence

Cells were fixed following the procedure of Hagan and Hyams (Hagan and Hyams, 1988) using glutaraldehyde and paraformaldehyde. In indirect immunofluorescence microscopy (Hagan and Yanagida, 1995), the SPB was stained with the anti-Sad1 antibody (a gift from O. Niwa, Kazusa DNA Research Institute, Kisatazu, Japan), microtubules were stained with the anti-α-tubulin antibody (TAT1). Subsequently, we added an Alexa-488-conjugated goat anti-mouse antibody (Molecular Probes, Eugene, OR) to label TAT1 or an Alexa-594-conjugated goat anti-rabbit antibody (Molecular Probes, Eugene, OR) to label anti-Sad1 antibody. The samples were then stained with 0.2 mg ml^{-1} Hoechst 33342 in PBS for 1 minute and mounted with antifade mounting medium containing 10 mg/ml *p*-phenylendiamine in 100 mM Tris-HCl (pH 8.8). Fluorescence images of these cells were observed using a fluorescence microscope (Olympus BX51) with a Cool SNAP CCD camera (Roper Scientific, San Diego, CA). Immunofluorescence images were acquired using Adobe Photoshop 7.0.

Results

Mcp6 is an *S.-pombe*-specific coiled-coil protein

Meu13 harbours a coiled-coil motif and plays a pivotal role in homologous pairing, meiotic recombination at meiosis I (Nabeshima et al., 2001) and the meiotic recombination checkpoint (Shimada et al., 2002). To identify a meiosis-specific coiled-coil protein of *S. pombe* that might interact with Meu13, we searched the genome database for uncharacterized genes that harbour coiled-coil motifs (http://www.sanger.ac.uk/Projects/S_pombe/) and found 60 genes. We then obtained DNA fragments from each of these genes and used them as probes for time-course northern blot analysis to examine their meiosis-specific

Fig. 1. Mcp6 is a meiosis-specific coiled-coil protein that harbours three homologous regions conserved in other proteins that are involved in the movement of subcellular components. (A) Schematic representation of Mcp6. The locations of the two coiled-coil motifs and the NLSs are indicated [as identified by PSORT II (http://psort.nibb.ac.jp/)]. (B) Schematic representation of Mcp6-related proteins of other species. The locations of homologous domains in these proteins are denoted by vertical white, grey and black arrowheads. Multiple sequence alignment shows homologous domains between Mcp6 from *S. pombe* (denoted *Sp*) and the related proteins from other species. Gaps inserted in the alignment to attain maximal homology are indicated by hyphens. The amino acids that are identical or similar among four or more of the seven species examined are shaded in black or grey. Abbreviations: MHC, myosin heavy chain; SMC, structural maintenance of chromosomes; Sp, *Schizosaccharomyces pombe*; At, *Arabidopsis thaliana*; Ce, *Caenorhabditis elegans*; Sc, *Saccharomyces cerevisiae*; Mm, *Mus musculus*; Xl, *Xenopus laevis*; Hs, *Homo sapiens*. The analysis of DNA sequences was performed by using the GENETYX program (Software Development, Tokyo, Japan). (C) Northern blot analysis of *mcp6*$^+$ and *aro3*$^+$ (loading control). Total RNA was extracted from *CD16-1* (h^+/h^-) and *CD16-5* (h^-/h^-) cells at the indicated times after the induction of meiosis by nitrogen starvation. RNA was blotted and probed with the ORFs of *mcp6*$^+$ and *aro3*$^+$. The graph below indicates the meiotic profiles of the cells used for RNA extraction. The progression of meiosis was monitored every 2 hours after nitrogen starvation. The numbers of cells that bear one, two, three or four nuclei were assessed by counting the nuclei stained with Hoechst 33342. At least 200 cells were counted under the microscope. (D) Western blot analysis of the production of Mcp6-GFP and Meu13 (meiotic timing control) proteins during the synchronous meiosis of strain ST194. Tubulin levels were also examined as a loading control.

transcription. This analysis identified seven novel *mcp* genes (Saito et al., 2004): *mcp1*$^+$ (AB189991); *mcp2*$^+$ (AB189990); *mcp3*$^+$ (AB189989); *mcp4*$^+$ (AB189988); *mcp5*$^+$ (AB189987); *mcp6*$^+$ (AB189986); *mcp7*$^+$ (AB189985).

Mcp6 consists of 327 amino acids and harbours two putative coiled-coil motifs, a leucine zipper (LZ), a nuclear localization signal (NLS), a peroxisomal targeting signal (PTS) and four potential Rad3-kinase phosphorylation target sites (SQ/TQ motifs) (Fig. 1A). Homology searches using the BLAST algorithm (at http://www.ncbi.nlm.nih.gov/BLAST/) indicate that Mcp6 is specific to *S. pombe*, because orthologues were not found in other organisms. Homology searching using the Block Maker program (http://bioinformatics.weizmann.ac.il/blocks/blockmkr/www/make_blocks.html) revealed that not only the coiled-coil domains but also other regions (depicted by filled vertical arrowheads) of Mcp6 are partly homologous to the myosin heavy chain (MHC), which is essential for cytokinesis (Rajagopalan et al., 2003) (Fig. 1B). Partial homology was also found with the SMC family of proteins, which are core components of the cohesin and condensin complexes that are required for chromosome movement (Jessberger, 2002). Moreover, we detected homology to Uso1, a protein required for endoplasmic-reticulum-to-Golgi vesicular transport in *Saccharomyces cerevisiae* (Sapperstein et al., 1996). A common functional feature of these proteins is their involvement in the dynamic movement of subcellular components. This suggests that Mcp6 might also be involved in subcellular dynamics.

The *mcp6*$^+$ gene is meiosis specific and expressed at the horsetail phase

To examine the meiosis-specific transcription of *mcp6*$^+$, we performed northern blot analyses of RNA obtained from CD16-1 (h^+/h^-) and CD16-5 (h^-/h^-) cells harvested at various times after the induction of meiosis by nitrogen starvation. In this experiment, we took advantage of the fact that the heterozygous CD16-1 strain initiates meiosis upon nitrogen starvation, whereas the homozygous CD16-5 strain does not. This analysis revealed that *mcp6*$^+$ displays meiosis-specific transcription that peaks at the horsetail phase (6 hours after induction), which is when homologous chromosome pairing and recombination occur (Fig. 1C).

When the Mcp6 protein appears during meiosis was then assessed by western blot analysis. To attain synchronous meiosis, we used the *pat1-114* temperature-sensitive strain, which enters meiosis in a highly synchronous manner when it is shifted to the restrictive temperature (Iino and Yamamoto, 1985). Thus, *pat1-114 mcp6*$^+$*-gfp* diploid cells that express Mcp6 protein tagged with GFP were induced to enter synchronized meiosis and their lysates were subjected to western blot analysis with an anti-GFP antibody. As shown in Fig. 1D, the frequency of horsetail nuclei is at a normal level, like the *pat1* control (Fig. 3A). Thus, we judged that the function of Mcp6-GFP is intact in this strain. Mcp6-GFP first appeared at the horsetail phase and its expression peaked at 3.5 hours after nitrogen starvation. This is similar to the timing of the production of Meu13 (Nabeshima et al., 2001). These results indicate that Mcp6 is a meiosis-specific protein that is exclusively expressed at the horsetail phase.

Mcp6 localizes to the SPB

We first examined the subcellular localization of Mcp6 by constructing a Mcp6-GFP-expressing strain in the h^{90} genetic background and inducing it to undergo meiosis by nitrogen starvation. As shown in the fluorescent microscope images in Fig. 2A (top), no GFP signal was detected during mitosis. Upon mating, however, the Mcp6-GFP fusion protein appeared as a dot near the edge of the nucleus during the horsetail period of meiosis (Fig. 2A, rows 2,

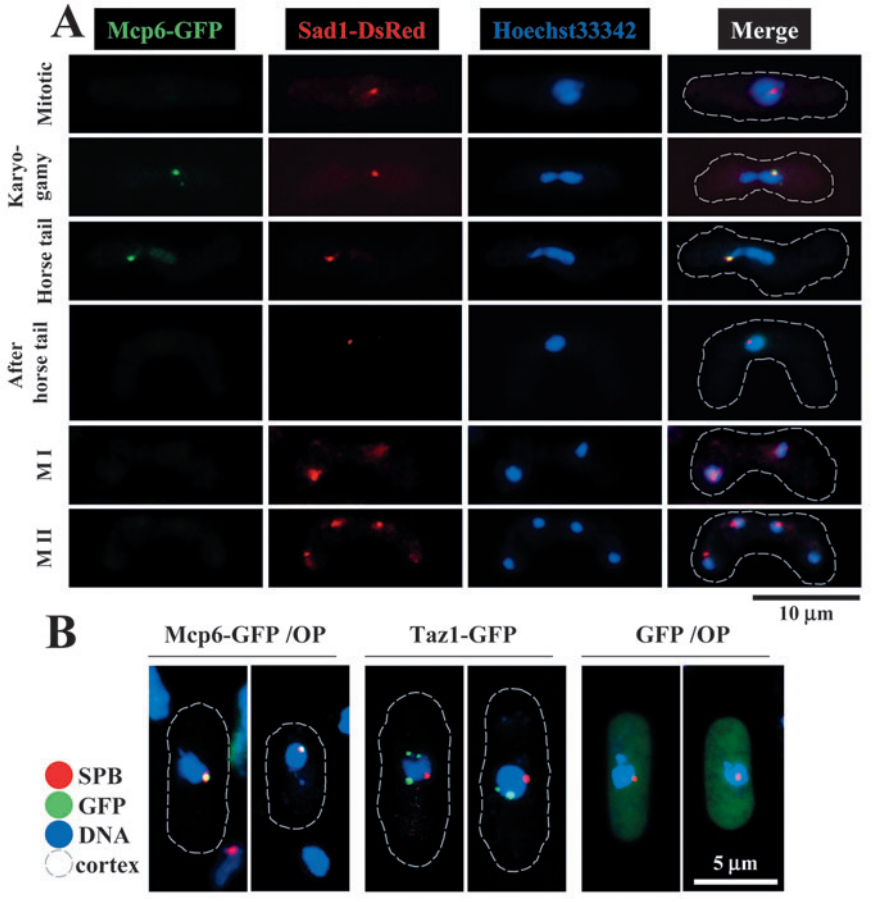

Fig. 2. Mcp6 is a meiosis-specific SPB-associated protein. (A) Microscopic analysis of Mcp6 localization during meiosis. The *mcp6*$^+$*-gfp dsred-sad1*$^+$ strain (ST142) was induced to enter meiosis by nitrogen starvation. After 6 hours of incubation, the cells were collected and fixed with methanol for microscopic observation. The GFP signal is green, the DsRed signal is red and Hoechst 33342 staining is blue. (B) Mcp6-GFP localizes to the SPB but not to the telomeres in mitotic cells. Overproduction by transforming mitotic cells with the pRGT81 (GFP expression vector) or *mcp6*$^+$/pRGT81 (Mcp6-GFP expression vector) plasmid is indicated by 'OP'.

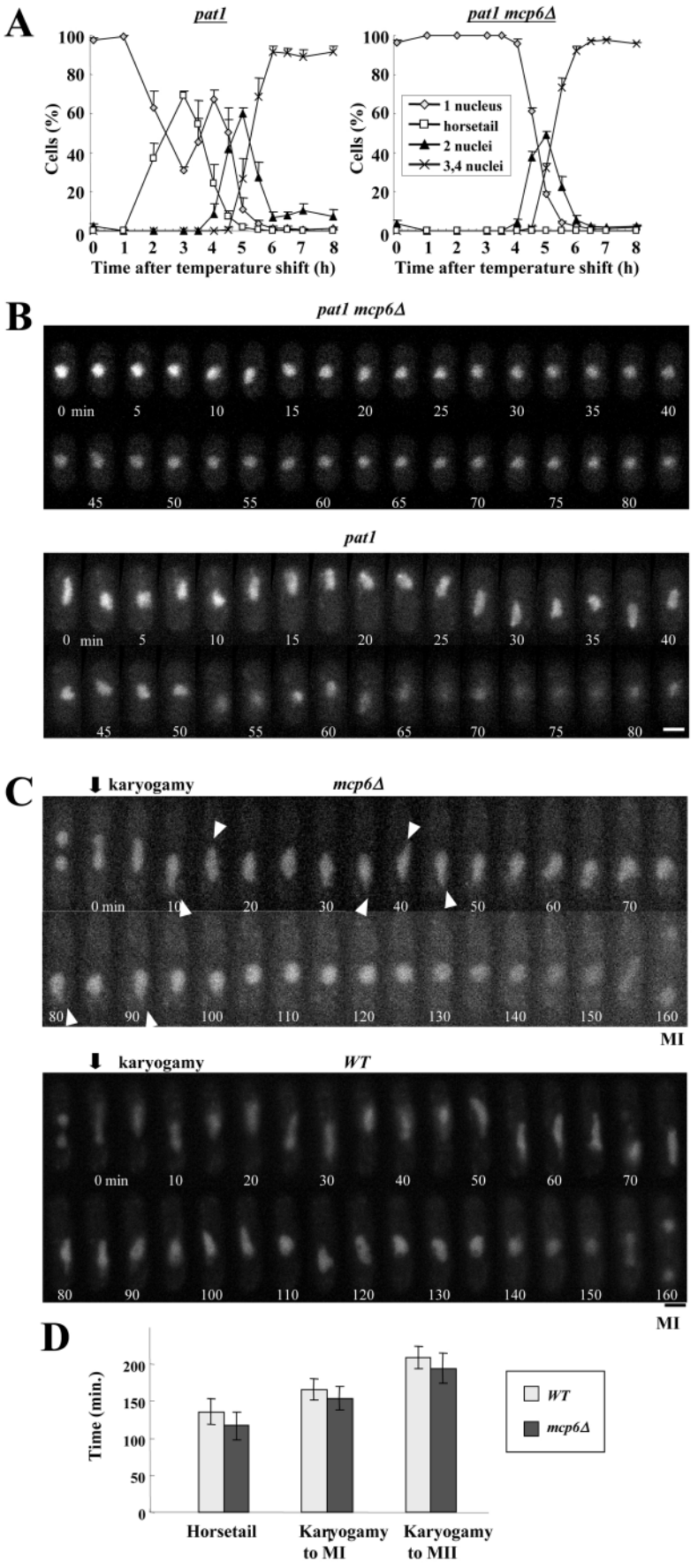

3). The dot disappeared after the horsetail period and the signal was not detected at meiosis I (MI) or meiosis II (MII). The dot localized with the fluorescence signal of Sad1-DsRed, which is known to localize to the SPB (Fig. 2A). Thus, Mcp6 is expressed only during the horsetail period of meiosis and might localize to the SPB.

Because the SPB and telomeres colocalize at this stage of meiosis, it was not clear whether Mcp6 localizes to the SPB or the telomeres. Thus, we expressed Mcp6-GFP (from the *nmt1* promoter in an expression vector pRGT81) and Sad1-DsRed (from the native promoter of *sad1*$^{+}$) during mitotic growth, which is when the SPB and telomeres localize to distinct subcellular loci. We confirmed that Sad1-DsRed does not localize with GFP-tagged Taz1, a component of telomeres, during mitosis (Fig. 2B). However, all of the Mcp6-GFP and Sad1-DsRed colocalized to the edge of the nucleus of the mitotic cells (Fig. 2B), which is where the SPB is known to be located. These results indicate that Mcp6 localizes to the SPB.

Nuclear movement during the meiotic prophase is hampered in the *mcp6Δ* mutant

To determine the role that Mcp6 plays in meiosis, we first examined the meiotic progression of *mcp6Δ* cells. To attain synchronous meiosis, we used the *pat1-114* temperature-sensitive strain again. Thus, homozygous

Fig. 3. Nuclear movement is abnormal during the horsetail phase in *mcp6Δ* cells. (A) Profiles of the meiotic progression in *pat1* (JZ670) and *pat1 mcp6Δ* (TT405) diploid cells (azygotic meiosis). The progression of meiosis was monitored every 30 minutes (3-7 hours) or 1 hour (0-2 hours and 7-8 hours) after the temperature shift, depending on the phase of meiosis. At least 200 cells were counted under a microscope to assess the frequencies of Hoechst-33342-stained cells that bear a horsetail, one nucleus, two nuclei and more than three nuclei. Each point denotes the average value of at least three independent experiments. Standard deviations are indicated as error bars. (B) Time-lapse images of *pat1* and *pat1 mcp6Δ* diploid cells during meiosis I. The nuclei were stained with Hoechst 33342. Images of a single cell were obtained at 2.5-minute intervals. The numbers at the bottom of each photograph represent the timing in minutes, with 0 minute being 2 hours after temperature shift to induce azygotic meiosis. Bar, 5 μm. (C) Time-lapse observation of wild-type (WT) (CT026-1) and *mcp6Δ* (ST193) cells during meiosis I. The nuclei were visualized by the fluorescence of a Polα-GFP fusion construct. Images of a single cell were obtained at 5 minute intervals. The numbers at the bottom of each photograph represent the timing in minutes, with 0 minutes being when nuclear fusion (karyogamy) occurs. The white arrowheads indicate the putative trailing edge of the moving nucleus. Bar, 5 μm. (D) The duration of meiotic prophase, meiosis I (MI) and meiosis II (MII) in *mcp6Δ* and WT cells. The average values were calculated from ten independent cells observed under a microscope. Standard deviations are shown as error bars.

diploid *pat1-114* cells were arrested at the G_1 phase by nitrogen starvation and then shifted to the restrictive temperature to induce synchronous meiosis. We then observed over time the number of nuclei in the cells of the *pat1-114* strain, whose *mcp6*$^+$ gene is intact, and in the cells of the *pat1-114 mcp6Δ* mutant. We found that the times at which cells with two or four nuclei peaked were similar for both strains (Fig. 3A).

Notably, almost no *pat1-114 mcp6Δ* cells (<0.5%) displayed the flat nuclear shape or the non-central position of the nucleus that are characteristic of the horsetail period. This is reminiscent of the description of the cells that bear a mutation in the SBP component Kms1 – that the nuclear shapes of these cells at prophase I of meiosis were aberrant (Shimanuki et al., 1997). Because the oscillatory nuclear movement that normally occurs during the prophase in wild-type meiosis (Chikashige et al., 1994) is impaired in the *kms1-null* mutant (Niwa et al., 2000), we surmised that deletion of *mcp6*$^+$ would also abolish nuclear migration. Thus, we examined over time the movement of chromosomes in *pat1-114 mcp6Δ* cells under a microscope. We found that horsetail oscillation at the prophase of meiosis I was indeed abrogated in these cells (Fig. 3B, top). In fact, almost no nuclear movement was observed throughout the prophase of meiosis in any of the *pat1-114 mcp6Δ* cells that we examined. By contrast, *pat1-114* cells displayed the marked nuclear oscillations that characterize this meiotic period (Fig. 3B, bottom).

Because the effects of mating and karyogamy cannot be observed at the restrictive temperature in the azygotic meiosis of *h*$^-$/*h*$^-$ *pat1-114* homozygous diploid cells, we also assessed the effect on nuclear oscillation of deleting the *mcp6*$^+$ gene in the *h*^{90} genetic background. Thus, we subjected these cells expressing Polα-GFP to time-lapse observation under a microscope. As shown in Fig. 3C (top), it is apparent that nuclear oscillation at prophase of meiosis I is also impaired in *mcp6Δ* cells. Notably, in contrast to *pat1-114 mcp6Δ* cells, slight movement was observed just after karyogamy, although no apparent movement was detected thereafter. The nucleus does seem to be moving a little in *mcp6Δ* cells because a trace of the trailing edge of the moving nucleus can be observed (Fig. 3B, white arrowheads). Nonetheless, it is evident that chromosomal movement is largely hampered in *mcp6Δ* cells compared with the vigorous nuclear movements in wild-type cells that occur several times after karyogamy (Fig. 3C, bottom).

Although it seems that the horsetail period (117 minutes) and the periods from karyogamy to meiosis I (154 minutes) and from karyogamy to meiosis II (195 minutes) in *mcp6Δ* cells were slightly shorter than those of wild-type cells (136 minutes, 166 minutes and 209 minutes, respectively) (Fig. 3D), these changes were not statistically

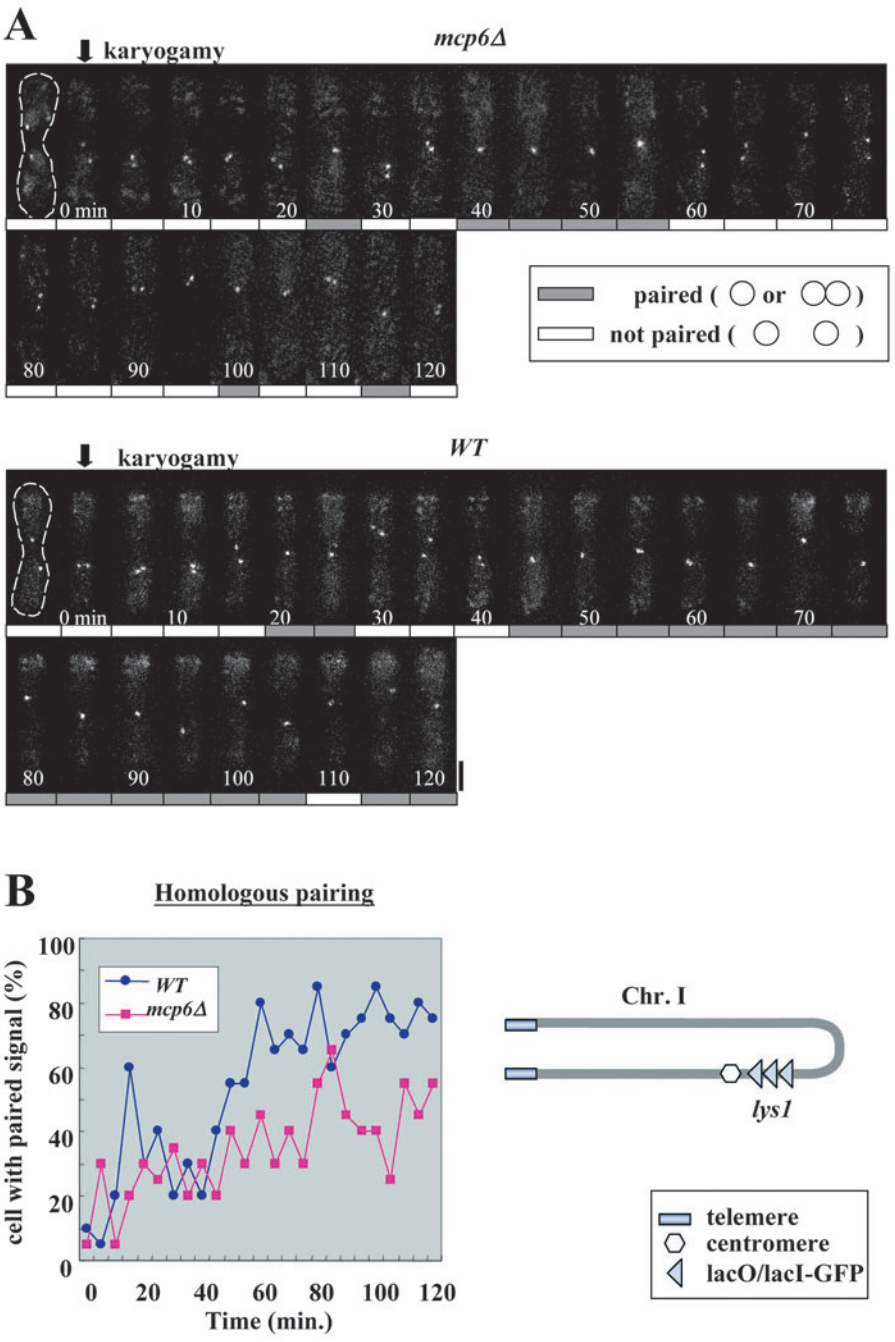

Fig. 4. Homologous pairing is reduced in *mcp6Δ* cells. (A) Time-lapse observation of the *lys1* locus in a living cell, either *mcp6Δ* (ST197) or wild type (WT) (AY174-7B), during the horsetail stage. The *lacO* repeat sequence integrated into the *lys1* loci was visualized by the LacI-NLS-GFP fusion protein. Images of a single cell were obtained at 5 minute intervals. The numbers at the bottom of each photograph represent the timing in minutes, with 0 minutes being when nuclear fusion (karyogamy) occurs. The rectangles under each photo indicate that the *lys1* loci were paired (grey) or not paired (white). Bar, 5 μm. (B) Time course of homologous pairing frequency during the horsetail stage in *mcp6Δ* (red square) compared with that in the WT (blue circle). The average values were calculated from 20 independent cells. The *lys1* locus in chromosome I is illustrated as an inset.

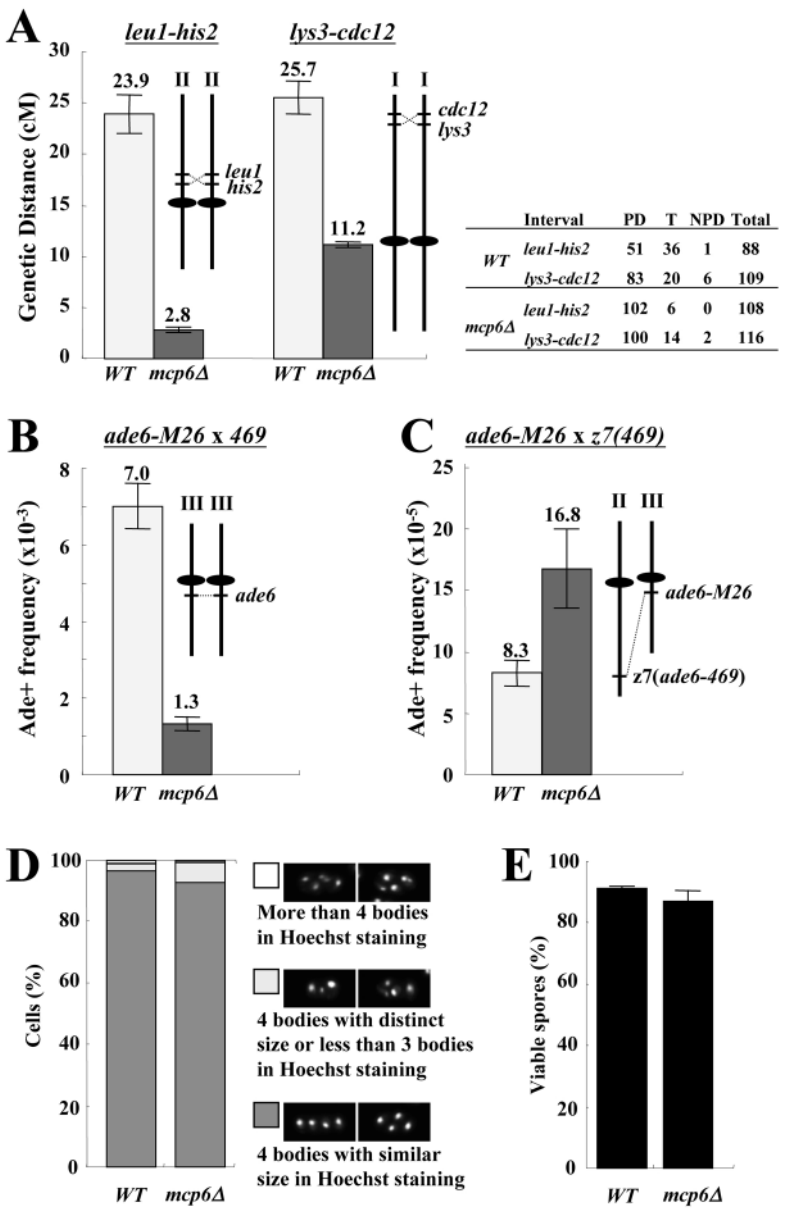

	Interval	PD	T	NPD	Total
WT	leu1-his2	51	36	1	88
	lys3-cdc12	83	20	6	109
mcp6Δ	leu1-his2	102	6	0	108
	lys3-cdc12	100	14	2	116

Fig. 5. Homologous recombination is reduced in *mcp6Δ* cells but ectopic recombination is increased compared with wild-type (WT) cells. The chromosomal positions of the loci and centromeres are illustrated in the insets. (A) Intergenic recombination (crossing over) showing the intervals between *leu1* and *his2* (left), *lys3* and *cdc12* (middle) and the primary tetrad (right). Only those tetrads that generated four viable spores were used to calculate the genetic distances (cM). The strains examined for *leu1-his2* crossing were WT (TT8-1 × NP32-2A) and *mcp6Δ* (TT398 × TT399), whereas the strains used for the *lys3-cdc12* crossing were WT (TT8-1 × TT231-1) and *mcp6Δ* (TT399 × TT411). The data shown are the average values calculated from at least three independent assays (at least 40 tetrads were dissected per assay). (B) Intragenic recombination. The strains examined were WT (MS105-1B × MS111w1) and *mcp6Δ* (TT400 × TT401). The average values were calculated from at least three independent assays. (C) Ectopic intragenic recombination. The strains crossed were WT (MS105-1B × GP1123) and *mcp6Δ* (TT400 × TT1014). The average values were calculated from at least three independent assays. Standard deviations are indicated as error bars. (D) Spores of *mcp6Δ* cells are almost normal as judged by the frequency of abnormal ascospores. The haploid parental strains were mated and sporulated on ME plate. After overnight culture, the cells were fixed with 70% ethanol for staining with Hoechst 33342. At least 200 cells were counted. (E) Spore viability of WT (TP4-5A × TP4-1D) and *mcp6Δ* (TT397-5A × TT397-1D) cells. Random spore analysis was performed.

significant (P>0.05 in Student's t-test). Thus, we conclude that the durations of the horsetail period, meiosis I and meiosis II are almost normal in h^{90} *mcp6Δ* cells (zygotic meiosis), as they are in the *pat1-114* genetic background (azygotic meiosis).

Homologous pairing is reduced in *mcp6Δ* cells

To investigate the requirement of Mcp6 in the process of chromosome pairing, we observed the homologous chromosomal regions in living zygotes during horsetail phase. By integrating a tandem repeat of the *Escherichia coli lac* operator sequence into the *S. pombe* genome at the *lys1*$^{+}$ locus (near the centromere of chromosome I), the fusion gene encoding GFP-LacI-NLS (which binds to the *lac* operator) was expressed in this strain. Consequently, two homologous loci on the chromosomes were visualized with GFP fluorescence (Nabeshima et al., 2001). In wild-type background, these homologous loci repeatedly associated and dissociated in the horsetail nucleus, oscillating back and forth between the cell poles (Fig. 4A, bottom). By contrast, the paired GFP signals were less frequent in *mcp6Δ* cells than in wild-type cells (Fig. 4A, top).

In order to quantify the pairing activity during the horsetail phase, we scored the occurrence of paired signals every 5 minutes from karyogamy to the first meiotic nuclear division in 20 live individuals of each strain. In the wild-type strain, the population of cells with paired signals during the initial 45 minutes was about 30% and then increased to about 80%. This level was maintained until 120 minutes (Fig. 4B, blue line). In *mcp6Δ* cells, there was no significant difference from the wild type in the initial 45 minutes but the subsequent increase in pairing observed in the wild type was completely absent (Fig. 4B, red line). These results indicate that Mcp6 is required for promoting homologous pairing with horsetail movement.

Meiotic recombination is abnormal in *mcp6Δ* cells

To determine whether, like the other SPB component Kms1, Mcp6 plays a role in meiotic recombination (Niwa et al., 2000), we compared the rates of intergenic and intragenic recombination in *mcp6Δ* and wild-type strains. We first investigated the crossover recombination of zygotic meiosis by tetrad analysis, which allowed us to measure the genetic distance between *leu1* and *his2* (Fig. 5A, insets). When the *mcp6Δ* strain was crossed, the genetic distance between *leu1* and *his2* was only 12% of the distance obtained when the wild-type strain was crossed (Fig. 5A, left). The genetic distances

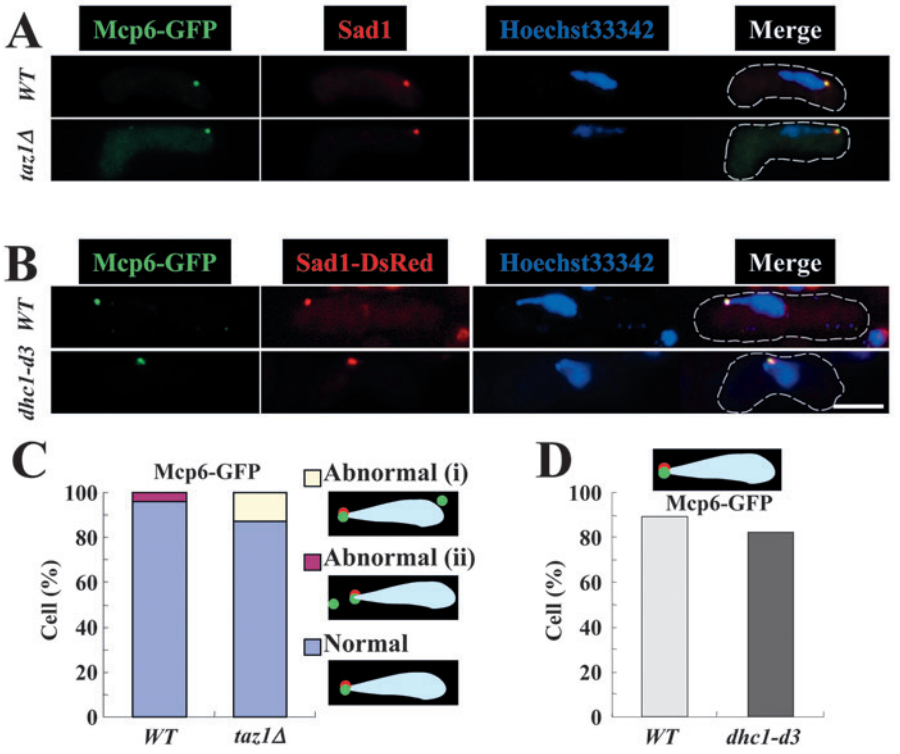

Fig. 6. The localization of Mcp6-GFP is normal in *taz1Δ* and *dhc1-d3* cells. (A) A typical immunofluorescence image of Mcp6-GFP at the horsetail phase in wild type (ST134) and *taz1Δ* (ST200) cells. (B) A typical image of Mcp6-GFP at the horsetail phase in wild-type (ST142) and *dhc1-d3* (ST196) cells (living). Bar, 5 μm. (C) Frequency of cells in which the Mcp6-GFP signals localize with Sad1 to the leading edge of the horsetail nucleus in the wild type and *taz1Δ* cells. (D) Frequency of cells in which the Mcp6-GFP signals localize with Sad1-DsRed to the leading edge of the horsetail nucleus in the wild-type and *dhc1-d3* cells.

between *lys3* and *cdc12* in the *mcp6Δ* strain was also reduced to 44% of that observed in the wild-type strain (Fig. 5A, right). We also characterized the intragenic recombination of the *mcp6Δ* strain between two different mutant alleles of *ade6* (*M26* and *469*). When the *mcp6Δ* strain was crossed, the frequency of Ade$^+$ recombinant spores was 19% of the wild-type frequency (Fig. 5B). Thus, it appears that Mcp6 plays a significant role in meiotic recombination.

To characterize the meiotic recombination competency of the *mcp6Δ* strain further, we examined the ectopic recombination rate. We used a pair of *ade6* alleles from different chromosomal loci, one at the natural position of *ade6* on chromosome III and the other at the *pac1* locus on chromosome II (*z7*) (Virgin and Bailey, 1998) (Fig. 5C). Notably, the frequency of ectopic recombination between these two loci in *mcp6Δ* cells was twice (202%) (in the *M26* and *469* pair) that of wild-type cells (Fig. 5C). A similar increase in the ectopic recombination rate between *M26* and *z15* (telomere of chromosome I) has been reported for the *kms1Δ* strain (Niwa et al., 2000). However, *mcp6Δ* cells are distinct from *kms1Δ* cells in that they do not display the abnormal telomere clustering that characterizes *kms1Δ* cells.

When we observed the spore morphology of *mcp6Δ* cells, we found that almost all of the spores looked normal (Fig. 5D). Indeed, depletion of Mcp6 caused only about 4% of the asci to display abnormal numbers of ascospores. The spore viability is also similar to that of wild-type cells (Fig. 5E). Thus, we conclude that Mcp6 does not play an important role in spore formation.

Taz1 and Dhc1 are not required for the localization of Mcp6 at the leading edge of the horsetail nucleus

In addition to chromosome oscillation at the horsetail phase, telomere clustering is required for the alignment and subsequent association of homologous chromosome arms (Ding et al., 2004). The telomere protein Taz1, whose deletion causes G_2/M-phase DNA-damage-checkpoint delay, chromosome mis-segregation and double-stranded DNA breaks, plays a role in preventing and repairing DNA breaks (Miller and Cooper, 2003) and telomere clustering (Cooper et al., 1998). To determine whether the SPB localization of Mcp6 depends on proper telomere clustering, we prepared *taz1* null mutant cells harbouring the integrated *mcp6*$^+$*-gfp* gene driven by its own promoter. These cells were then induced to enter meiosis by nitrogen starvation and the Mcp6-GFP signal was observed by immunofluorescence. As shown in Fig. 6A,C, the subcellular localization of Mcp6-GFP was almost normal in *taz1Δ* cells (71 cells were counted in both wild-type and *mcp6Δ* cells).

We next examined whether SPB localization of Mcp6 is dependent on dynein. To do this, we prepared a *dhc1-d3* mutant harbouring the integrated *mcp6*$^+$*-gfp* gene driven by its own promoter and induced it to enter meiosis by nitrogen starvation. Mcp6-GFP colocalized normally with DsRed-Sad1 to the SPB in *dhc1-d3* cells, which suggests that Dhc1 is not required for the proper localization of Mcp6 at the SPB (Fig. 6B). The frequency of cells in which Sad1-DsRed and Mcp6-GFP colocalized to the leading edge of the horsetail nucleus was 94% (15/18) in *dhc1-d3* cells, which is almost equal to the frequency in wild-type cells (93%; 32/36) (Fig. 6D).

Subcellular localization of SPB components is normal in *mcp6Δ* cells

For proper horsetail movement, it is essential that the telomeres cluster at the SPB after karyogamy and that the telomere/SPB complex migrates on the microtubule that radially extends from the SPB to the cell cortex on the opposite site of the cell. To understand the role of Mcp6 in horsetail movement, we examined the subcellular localization of the SPB components Sad1, Spo15 and Kms1 in *mcp6Δ* cells. Sad1 is a constitutive component of SPB that is essential for normal bipolar spindle formation (Hagan and Yanagida, 1995), Spo15 is associated with SPBs throughout the life cycle and plays an indispensable role in the initiation of spore membrane formation (Ikemoto et

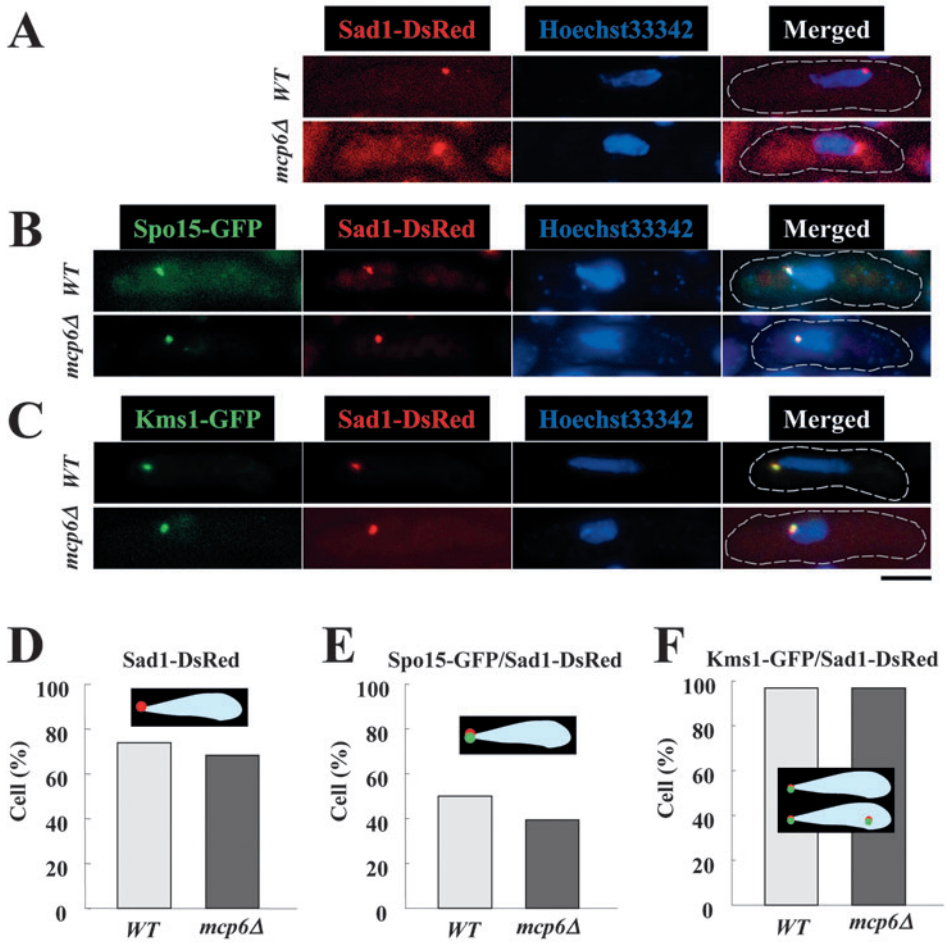

Fig. 7. The subcellular localization of GFP-tagged SPB components at the horsetail phase is normal in *mcp6Δ* cells. The h^{90} strains that express Sad1-DsRed (WT, CRL790; *mcp6Δ*, ST148) (A), Spo15-GFP (*WT*, ST176; *mcp6Δ*, ST171-1) (B) or Kms1-GFP (*WT*, ST191-1; *mcp6Δ*, ST172-1) (C) fusion proteins were induced to enter meiosis by nitrogen starvation. After 6 hours, the cells were collected and observed under a fluorescence microscope. Typical images are shown. (D) The proportions of the cell population in which Sad1-DsRed localized to the leading edge of the nucleus with a single dot, as depicted in the inset. (E) The proportions of the cell population in which Spo15-GFP and Sad1-DsRed colocalized to the leading edge of the nucleus with a single dot, as depicted in the inset. (F) The proportions of the cell population in which Kms1-GFP and Sad1-DsRed colocalized to the leading edge of the nucleus, as depicted in the inset. Green, GFP; red, Sad1-DsRed; blue, Hoechst 33342. The dotted line depicts the contour of the cell. Bar, 5 μm.

al., 2000), and Kms1 is required for the formation of meiotic prophase-specific nuclear architecture (Shimanuki et al., 1997). To do this, we prepared strains that express the Sad1-dsRed protein and the other GFP-fused components from their own promoters in the *mcp6-null* genetic background. The cells were induced to enter meiosis by nitrogen starvation and then observed under a fluorescence microscope.

We first investigated the localization of Sad1-dsRed during the horsetail phase and found that, in *mcp6Δ* cells, 68% (17/25) of the Sad1 signal constituted a single dot at the leading edge of the nucleus (Fig. 7A,D). This is similar to what is observed in wild-type cells (59/82, or 72%, of the Sad1 signal is present as a single dot). These results indicate that Mcp6 is not required for Sad1 localization to the SPB. We next examined the localization of Spo15-GFP and found that most of the Spo15 signal localized with Sad1-DsRed to the SPB in both *mcp6Δ* and wild-type cells (Fig. 7B,E). We also examined the localization of Kms1-GFP and found that most Kms1-GFP and Sad1-DsRed colocalized to either the SPB or the Sad1 body in both *mcp6Δ* and wild-type cells (Fig. 7C,F). These results indicate that Mcp6 is not required for the proper organization of SPB architecture.

Telomere localization is normal but microtubule organization is abnormal in *mcp6Δ* cells

Telomere clustering near the SPB, which occurs during the prophase of meiosis I, is an essential event for efficient chromosome pairing and cells deficient in the telomere-associated protein Taz1 (*taz1Δ*) have been reported to have defective telomere clustering, reduced recombination rates, abnormal spore formation and reduced spore viability (Nimmo et al., 1998; Cooper et al., 1998). To determine whether telomere clustering is normal in *mcp6Δ* cells, we examined the subcellular localization of the telomere proteins Taz1 and Swi6 by preparing h^{90} *taz1*$^{+}$*-gfp sad1*$^{+}$*-dsred* and h^{90} *swi6*$^{+}$*-gfp sad1*$^{+}$*-dsred* strains, which express Sad1-dsRed together with GFP-tagged Taz1 or Swi6 from their own promoters. These strains were induced to enter meiosis by nitrogen starvation and then observed under a fluorescence microscope. The Taz1-GFP signal of the telomere at the leading edge of the nucleus localized with the Sad1-DsRed signal to the SPB in 62% (23/37) and 58% (14/24) of the *mcp6Δ* and wild-type cells, respectively (Fig. 8A,D). The Swi6-GFP signal also localized with the Sad1-DsRed signal to the SPB at similar levels in *mcp6Δ* (76%; 13/17) and wild-type cells (85%; 35/41) (Fig. 8B). These results indicate that the subcellular localization of Taz1 and Swi6 is normal in *mcp6Δ* cells – namely, Mcp6 is required for neither SPB organization nor telomere clustering.

The oscillatory nuclear movement is mediated by dynamic reorganization of astral microtubules originating from the SPB. To observe the organization of microtubules in *mcp6Δ* cells, we prepared the h^{90} strain that expresses GFP-fused α-tubulin from the *nmt1* promoter. After 6 hours' induction of meiosis

in EMM2-N medium, the strain was fixed with glutaraldehyde and paraformaldehyde for immunostaining. In wild-type cells, 95% (156/165) of astral microtubules originated from the SPB during the horsetail phase. In *mcp6Δ* cells, however, collapse of astral microtubule organization was observed (Fig. 8C,F): 21% (21/100) of *mcp6Δ* cells displayed the microtubules not associated with SPB [Fig. 8F, abnormal (i)]. We also found that 60% (60/100) of *mcp6Δ* cells showed abnormal astral microtubules that originated from the SBP but branched elsewhere [Fig. 8F; abnormal (ii)]. These results indicate that Mcp6 is required for proper astral microtubule positioning during horsetail phase.

Discussion

Mcp6 is required for horsetail movement of chromosomes

In the present study, we show that Mcp6 is a novel coiled-coil protein that is only expressed during the horsetail period of meiosis (Fig. 1) and localizes to the SPB (Fig. 2). We found that the deletion of *mcp6*$^{+}$ almost abolished horsetail movement of chromosomes (Fig. 3) and reduced recombination rates (Fig. 5). Notably, we observed that, whereas deletion of *mcp6*$^{+}$ from the homozygous diploid *pat1* genetic background completely abolished horsetail movement during azygotic meiosis of these cells (Fig. 3B), a slight chromosome movement after karyogamy was observed during the zygotic meiosis of *mcp6Δ* cells in the h^{90} genetic background (Fig. 3C). This indicates that karyogamy is important for initiating horsetail movement and suggests that Mcp6 plays a role during or just after karyogamy. BLAST-based homology searches failed to identify proteins in other species that are homologous to Mcp6. Thus, Mcp6 is an *S.-pombe*-specific protein. This is reasonable because *S. pombe* is the only organism examined so far that displays horsetail movement of nucleus.

Two *S. pombe* mutants [*kms1-1* (Shimanuki et al., 1997; Niwa et al., 2000) and *dhc1* mutants (Yamamoto et al., 1999)] have been reported to lack horsetail movement. Another mutant (*dlc1Δ*) also shows abnormal horsetail movement (Miki et al., 2002). Although Kms1, which is also an *S.-pombe*-specific protein, localizes to the SPB throughout mitotic and meiotic phases, abnormal phenotypes of *kms1-1* cells are only detected in meiosis (Niwa et al., 2000). Dhc1, the dynein heavy chain that is conserved among various species, localizes to the SPB, microtubules and cell cortex, and is predominantly expressed from karyogamy through to meiosis I (Yamamoto et al., 1999). Thus, Mcp6 is a new

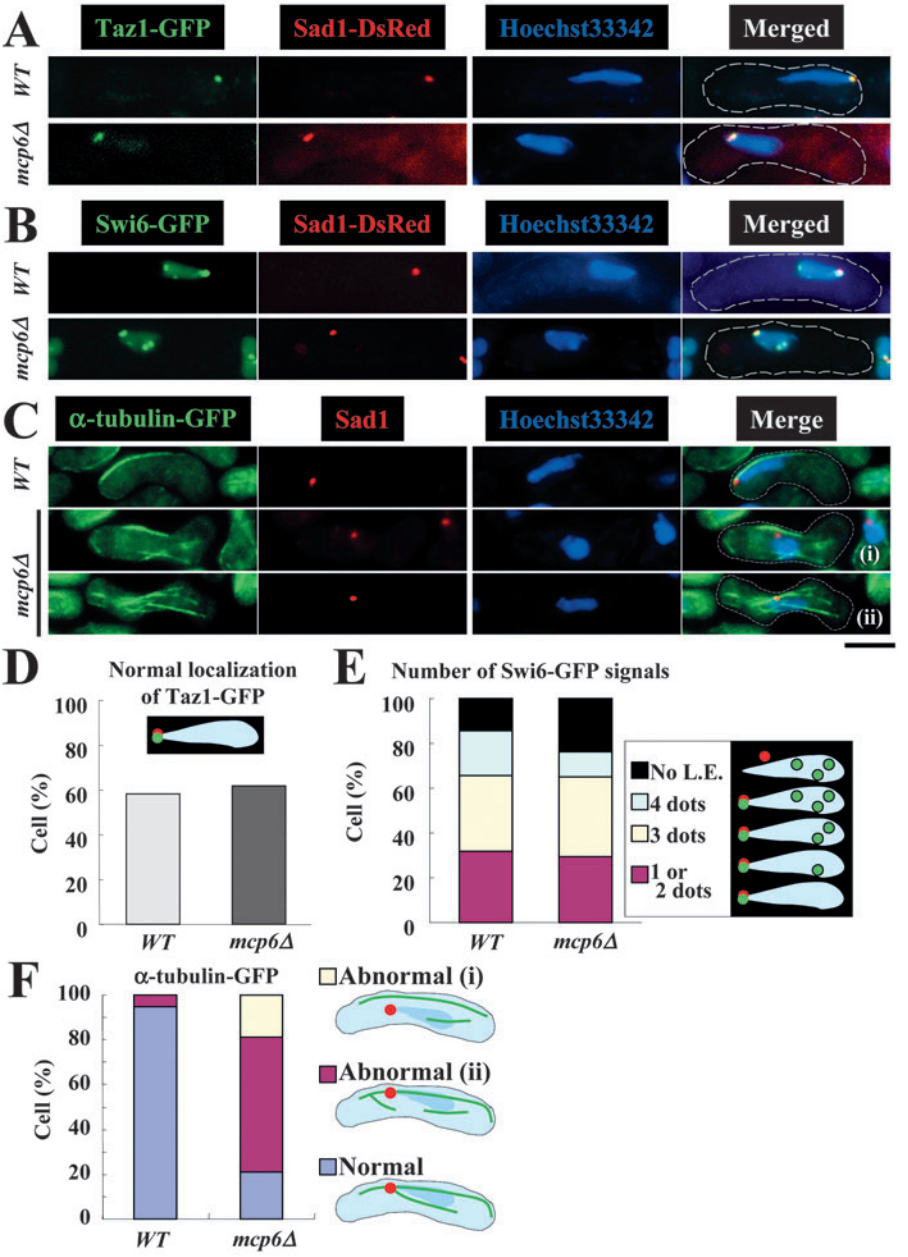

Fig. 8. GFP-tagged telomere components and α-tubulin localize normally in *mcp6Δ* cells. The h^{90} strains that express Taz1-GFP (*WT*, ST178; *mcp6Δ*, ST173) (A), Swi6-GFP (*WT*, ST179-1; *mcp6Δ*, ST174) (B) or α-tubulin-GFP (*WT*, YY105; *mcp6Δ*, ST146) (C) were induced to enter meiosis by nitrogen starvation. After 6 hours, the cells were collected and observed under a fluorescence microscope. Images shown in (C) were obtained by immunofluorescence. Typical images are shown. (D) The proportions of the cell population in which Taz1-GFP and Sad1-DsRed colocalized to the leading edge of the nucleus with a single dot, as depicted in the inset. (E) The proportions of the cell population in which Swi6-GFP and Sad1-DsRed colocalized to the leading edge (L.E.) of the nucleus with extra dots of Swi6-GFP in the nucleus, as depicted in the insets. (F) The proportions of the cell population that display normal or abnormal (i) and (ii) tubulin positioning as depicted on the right. Green, GFP; red, Sad1-DsRed (A,B) or Sad1 (C); blue, Hoechst 33342. The dotted line indicates the contour of the cell. Bar, 5 μm.

member of this group of SPB- and horsetail-movement-associated proteins. In support of this, *mcp6Δ* cells show similar phenotypes to the *kms1-1*, *kms1Δ*, *dhc1* and *dlc1Δ* mutant cells as follows. First, like *kms1*, *dhc1* and *dlc1Δ* mutants, the rates of intergenic or intragenic recombination of the *mcp6Δ* mutant are markedly reduced (Fig. 5A,B). Second, the ectopic recombination rate of *mcp6Δ* cells is increased about twofold (Fig. 5C), as has also been observed for the ectopic recombination of *kms1Δ* cells between *ade6-M26* and *ade6-469* (*z15*) loci, although the rate of ectopic recombination between the *ade6-M26* and *ade6-469* (*z7*) loci in *kms1Δ* cells was almost the same as that in wild-type cells (Niwa et al., 2000).

However, Mcp6 does have some phenotypes that differ from those of *kms1*, *dhc1* and *dlc1Δ* mutants, and thus it seems to play a distinct role in maintaining the horsetail movement. One such phenotype is the almost normal spore formation and spore viability in *mcp6Δ* cells (Fig. 5D,E). By contrast, spore formation and spore viability are abnormal in *kms1Δ*, *dhc1Δ* and *dlc1Δ* cells. Second, unlike *kms1Δ* cells (Shimanuki et al., 1997), telomere clustering, as determined by examining the subcellular localization of Taz1-GFP and Swi6-GFP, appears almost normal in *mcp6Δ* cells (Fig. 8). Third, although *kms1Δ* and *dhc1-d3* cells showed reduced SPB integrity and abnormal chromosome segregation, respectively, the *mcp6Δ* mutant does not show such abnormalities (Figs 6, 7). Fourth, Mcp6 is the only meiosis-specific protein of this group, because Kms1, Dhc1 and Dlc1 are also detected in both the mitotic and meiotic phases (Goto et al., 2001; Miki et al., 2002).

Mcp6 plays a role in homologous pairing by regulating horsetail movement

We report here that recombination rates are greatly reduced in *mcp6Δ* cells compared with wild-type cells (Fig. 5), which is due primarily to the inefficient homologous pairing of chromosomes in *mcp6Δ* cells (Fig. 4). This inefficient homologous pairing is mainly derived from the impaired horsetail movement of nucleus (Fig. 3). We previously showed that *meu13Δ* and *mcp7Δ* cells show a delay in entering meiosis I, and that this is due to the meiotic recombination checkpoint that provides cells with enough time to repair double-strand breaks (DSBs) in a manner dependent on checkpoint *rad*$^{+}$ genes (Shimada et al., 2002; Saito et al., 2004). In the case of *mcp6Δ* cells, however, even though recombination rates were reduced, a delay in entering meiosis I was not observed (Fig. 3A). Thus, we surmise that Mcp6 is not involved in DSB repair like other SPB components, probably because Mcp6 is located at the SPB, a location that is too remote directly to regulate DSBs on chromatin. Similarly, Mcp6 might not directly regulate the recombination machinery. Thus, it is most probable that Mcp6 is involved in regulating the pairing of homologous chromosomes by inducing proper horsetail movement.

Mcp6 is a novel type of regulator of horsetail movement

Some mutants (*lot2-s17*, *lot3-uv3/taz1*, *dot1* and *dot2*) show defective horsetail movement and reduced meiotic recombinations, but their phenotypes are distinct from *mcp6Δ*. For example, *lot2-s17* and *lot3-uv3/taz1* mutants display a dramatic lengthening of telomeric repeats, low spore viability and chromosome mis-segregation through meiosis (Nimmo et al., 1998; Cooper et al., 1998; Hiraoka et al., 2000). Two mutants (*dot1* and *dot2*) do not sporulate and show defective SPB integrity and impaired telomere clustering (Jin et al., 2002). By contrast, we show here that *mcp6Δ* differs from these mutants because sporulation (Fig. 5D,E), SPB integrity (Fig. 7) and telomere clustering (Fig. 6) are almost normal.

Some mutant strains of *taz1* that show abnormal horsetail movement (Hiraoka et al., 2000) are also distinct from *mcp6Δ* cells. First, telomere clustering is abnormal in *taz1Δ* cells. Second, *taz1Δ* cells display abnormal spore formation and reduced spore viability. Third, although the subcellular localization of Taz1-GFP is normal in *mcp6Δ* cells (Fig. 8A), Mcp6-GFP localization became slightly abnormal in *taz1Δ* cells (Fig. 6A,C). Thus, Mcp6 might interact with Taz1 but its role in chromosome maintenance during meiosis is quite distinct.

Finally, microtubules are nucleated exclusively from SPBs immediately after karyogamy and form typical X-shaped configurations during nuclear fusion of meiotic cells (Svoboda et al., 1995; Yamamoto et al., 1999). However, we report here that the astral microtubule organization was largely abnormal in *mcp6Δ* cells (Fig. 8). Thus, in the absence of Mcp6, many cells fail to organize a long, curved microtubule array that extends from the cell ends to provide the tracks for nuclear horsetail movement, resulting in the abolished nuclear oscillation and reduced chromosome pairing. Taken together, we conclude that Mcp6 controls horsetail movement by regulating the astral microtubule organization during meiosis.

We thank O. Niwa, Y. Hiraoka, A. Yamamoto, C. Shimoda, M. Yamamoto, G. R. Smith, K. M. Miller and W. Z. Cande for providing *S. pombe* strains, and O. Niwa for the anti Sad1 antibody. We also thank K. Nabeshima for technical advice in the experiments of chromosome pairing, E. Okamura for technical assistance, and P. Hughes for critically reading the manuscript. This work was supported by a Grant-in-aid for Scientific Research on Priority Areas from the Ministry of Education, Science, Sports and Culture of Japan and a grant from the Uehara Memorial Foundation to H.N.

References

Alfa, C., Fantes, P., Hyams, J., McLeod, M. and Warbrick, E. (1993). *Experiments with Fission Yeast: A laboratory course manual.* Cold Spring Harbor Laboratory Press, Cold Spring Harbor, NY, USA.

Burkhard, P., Stetefeld, J. and Strelkov, S. V. (2001). Coiled coils: a highly versatile protein folding motif. *Trends Cell Biol.* **11**, 82-88.

Chikashige, Y., Ding, D. Q., Funabiki, H., Haraguchi, T., Mashiko, S., Yanagida, M. and Hiraoka, Y. (1994). Telomere-led premeiotic chromosome movement in fission yeast. *Science* **264**, 270-273.

Chikashige, Y., Ding, D. Q., Imai, Y., Yamamoto, M., Haraguchi, T. and Hiraoka, Y. (1997). Meiotic nuclear reorganization: switching the position of centromeres and telomeres in the fission yeast *Schizosaccharomyces pombe*. *EMBO J.* **16**, 193-202.

Cooper, J. P., Watanabe, Y. and Nurse, P. (1998). Fission yeast Taz1 protein is required for meiotic telomere clustering and recombination. *Nature* **392**, 828-831.

Ding, D. Q., Chikashige, Y., Haraguchi. T. and Hiraoka, Y. (1998). Oscillatory nuclear movement in fission yeast meiotic prophase is driven by astral microtubules, as revealed by continuous observation of chromosomes and microtubules in living cells. *J. Cell Sci.* **111**, 701-712.

Ding, D. Q., Tomita, Y., Yamamoto, A., Chikashige, Y., Haraguchi, T. and Hiraoka, Y. (2000). Large-scale screening of intracellular protein localization in living fission yeast cells by the use of a GFP-fusion genomic DNA library. *Genes Cells* **5**, 169-190.

Ding, D. Q., Yamamoto, A., Haraguchi, T. and Hiraoka, Y. (2004). Dynamics of homologous chromosome pairing during meiotic prophase in fission yeast. *Dev. Cell* **6**, 329-341.

Fukushima, K., Tanaka, Y., Nabeshima, K., Yoneki, T., Tougan, T., Tanaka, S. and Nojima, H. (2000). Dmc1 of *Schizosaccharomyces pombe* plays a role in meiotic recombination. *Nucleic Acids Res.* **28**, 2709-2716.

Goto, B., Okazaki, K. and Niwa, O. (2001). Cytoplasmic microtubular system implicated in de novo formation of a Rabl-like orientation of chromosomes in fission yeast. *J. Cell Sci.* **114**, 2427-2435.

Grimm, C., Kohli, J., Murray, J. and Maundrell, K. (1988). Genetic engineering of *Schizosaccharomyces pombe*: a system for gene disruption and replacement using the ura4 gene as a selectable marker. *Mol. Gen. Genet.* **215**, 81-86.

Gutz, H. (1971). Gene conversion: remarks on the quantitative implications of hybrid DNA models. *Genet. Res.* **17**, 45-52.

Hagan, I. and Hyams, S. J. (1988). The use of cell division cycle mutants to investigate the control of microtubule distribution in the fission yeast *Schizosaccharomyces pombe*. *J. Cell Sci.* **89**, 343-357.

Hagan, I. and Yanagida, M. (1995). The product of the spindle formation gene *sad1*$^{+}$ associates with the fission yeast spindle pole body and is essential for viability. *J. Cell Biol.* **129**, 1033-1047.

Hiraoka, Y. (1998). Meiotic telomeres: a matchmaker for homologous chromosomes. *Genes Cells* **3**, 405-413.

Hiraoka, Y., Ding, D. Q., Yamamoto, A., Tsutsumi, C. and Chikashige, Y. (2000). Characterization of fission yeast meiotic mutants based on live observation of meiotic prophase nuclear movement. *Chromosoma* **109**, 103-109.

Ikemoto, S., Nakamura, T., Kubo, M. and Shimoda, C. (2000). *S. pombe* sporulation-specific coiled-coil protein Spo15p is localized to the spindle pole body and essential for its modification. *J. Cell Sci.* **113**, 545-554.

Iino, Y. and Yamamoto, M. (1985). Mutants of *Schizosaccharomyces pombe* which sporulate in the haploid state. *Mol. Gen. Genet.* **198**, 416-421.

Jin, Y., Uzawa, S. and Cande, W. Z. (2002). Fission yeast mutants affecting telomere clustering and meiosis-specific spindle pole body integrity. *Genetics* **160**, 861-876.

Jessberger, R. (2002). The many functions of SMC proteins in chromosome dynamics. *Nat. Rev. Mol. Cell Biol.* **10**, 767-778.

Kanoh, J. and Ishikawa, F. (2001). spRap1 and spRif1, recruited to telomeres by Taz1, are essential for telomere function in fission yeast. *Curr. Biol.* **11**, 1624-1630.

Kohli, J. (1994). Meiosis. Telomeres lead chromosome movement. *Curr. Biol.* **4**, 724-727.

Loidl, J. (1990). The initiation of meiotic chromosome pairing: the cytological view. *Genome* **33**, 759-778.

Miki, F., Okazaki, K., Shimanuki, M., Yamamoto, A., Hiraoka, Y. and Niwa, O. (2002). The 14-kDa dynein light chain-family protein Dlc1 is required for regular oscillatory nuclear movement and efficient recombination during meiotic prophase in fission yeast. *Mol. Biol. Cell* **13**, 930-946.

Miller, K. M. and Cooper, J. P. (2003). The telomere protein Taz1 is required to prevent and repair genomic DNA breaks. *Mol. Cell* **11**, 303-313.

Nabeshima, K., Kakihara, Y., Hiraoka. Y. and Nojima, H. (2001). A novel meiosis-specific protein of fission yeast, Meu13p, promotes homologous pairing independently of homologous recombination. *EMBO J.* **20**, 3871-3881.

Nimmo, E. R., Pidoux, A. L., Perry, P. E. and Allshire, R. C. (1998). Defective meiosis in telomere-silencing mutants of *Schizosaccharomyces pombe*. *Nature* **392**, 825-828.

Niwa, O., Shimanuki, M. and Miki, F. (2000). Telomere-led bouquet formation facilitates homologous chromosome pairing and restricts ectopic interaction in fission yeast meiosis. *EMBO J.* **19**, 3831-3840.

Okuzaki, D., Satake, W., Hirata, A. and Nojima, H. (2003). Fission yeast *meu14*$^{+}$ is required for proper nuclear division and accurate forespore membrane formation during meiosis II. *J. Cell Sci.* **116**, 2721-2735.

Perkins, D. D. (1949). Biochemical mutants in smut fungus *Ustilago maydis*. *Genetics* 34, 607-626.

Rajagopalan, S., Wachtler, V. and Balasubramanian, M. (2003). Cytokinesis in fission yeast: a story of rings, rafts and walls. *Trends Genet.* **19**, 403-408.

Saito, T. T., Tougan, T., Kasama, T., Okuzaki, D. and Nojima, H. (2004). Mcp7, a meiosis-specific coiled-coil protein of fission yeast, associates with Meu13 and is required for meiotic recombination. *Nucleic Acids Res.* **32**, 3325-3339.

Sapperstein, S. K., Lupashin, V. V., Schmitt, H. D. and Waters, M. G. (1996). Assembly of the ER to Golgi SNARE complex requires Uso1p. *J. Cell Biol.* **132**, 755-767.

Scherthan, H. (2001). A bouquet makes ends meet. *Nat. Rev. Mol. Cell Biol.* **2**, 621-627.

Shimanuki, M., Miki, F., Ding, D. Q., Chikashige, Y., Hiraoka, Y., Horio, T. and Niwa, O. (1997). A novel fission yeast gene, *kms1*$^{+}$, is required for the formation of meiotic prophase-specific nuclear architecture. *Mol. Gen. Genet.* **254**, 238-249.

Shimada, M., Nabeshima, K., Tougan, T. and Nojima, H. (2002). The meiotic recombination checkpoint is regulated by checkpoint *rad*$^{+}$ genes in fission yeast. *EMBO J.* **21**, 2807-2818.

Sipiczki, M. and Ferenczy, L. (1977). Protoplast fusion of *Schizosaccharomyces pombe* auxotrophic mutants of identical mating-type. *Mol. Gen. Genet.* **151**, 77-81.

Svoboda, A., Bahler, J. and Kohli, J. (1995). Microtubule-driven nuclear movements and linear elements as meiosis-specific characteristics of the fission yeasts *Schizosaccharomyces versatilis* and *Schizosaccharomyces pombe*. *Chromosoma* **104**, 203-214.

Virgin, J. B. and Bailey, J. P. (1998). The M26 hotspot of *Schizosaccharomyces pombe* stimulates meiotic ectopic recombination and chromosomal rearrangements. *Genetics* **149**, 1191-1204.

Watanabe, T., Miyashita, K., Saito, T. T., Yoneki, T., Kakihara, Y., Nabeshima, K., Kishi, Y. A., Shimoda, C. and Nojima, H. (2001). Comprehensive isolation of meiosis-specific genes identifies novel proteins and unusual non-coding transcripts in *Schizosaccharomyces pombe*. *Nucleic Acids Res.* **29**, 2327-2337.

Yamamoto, A. and Hiraoka, Y. (2001). How do meiotic chromosomes meet their homologous partners?: lessons from fission yeast. *BioEssays* **23**, 526-533.

Yamamoto, A. and Hiraoka, Y. (2003). Cytoplasmic dynein in fungi: insights from nuclear migration. *J. Cell Sci.* **116**, 4501-4512.

Yamamoto, A., West, R. R., McIntosh, J. R. and Hiraoka, Y. (1999). A cytoplasmic dynein heavy chain is required for oscillatory nuclear movement of meiotic prophase and efficient meiotic recombination in fission yeast. *J. Cell Biol.* **145**, 1233-1249.

Yamamoto, A., Tsutsumi, C., Kojima, H., Oiwa, K. and Hiraoka, Y. (2001). Dynamic behavior of microtubules during dynein-dependent nuclear migrations of meiotic prophase in fission yeast. *Mol. Biol. Cell* **12**, 3933-3946.

Zickler, D. and Kleckner, N. (1999). Meiotic chromosomes: integrating structure and function. *Annu. Rev. Genet.* **33**, 603-754.